Functionalization of CPO-27-Ni through metal hexacarbonyls: The role of open Ni2+ sites

Functionalization of CPO-27-Ni through metal hexacarbonyls: The role of open Ni^{2+} sites

Sachin Chavan[a], Jenny G. Vitillo[a], Elena Groppo[a], M. Cherif Larabi[b], E. Alessandra Quadrelli[b], Pascal D.C. Dietzel[c] and Silvia Bordiga[a]**

[a]Department of Inorganic, Physical and Material Chemistry, University of Torino, via Giuria 7, 10125 Torino, and NIS Centre of Excellence and INSTM Centro di Riferimento, via Quarello 11, I-10135, Torino (Italy).

[b]Université de Lyon, Institut de Chimie de Lyon ; UCBL1- CPE Lyon -CNRS, UMR 5265 C2P2, LCOMS Boulevard du 11 Novembre 1918 F-69616, Villeurbanne, France.

[c]SINTEF Materials and Chemistry, Postboks 124, Blindern, N-0314, Oslo, Norway, Centre for Materials Science and Nanotechnology, Department of Chemistry, University of Oslo, Postboks 1033, Blindern, N-0315, Oslo, Norway

Corresponding authors: Silvia Bordiga: silvia.bordiga@unito.it. and E. Alessandra Quadrelli: aquadrelli@cpe.fr

Abstract

$Cr(CO)_6$ and $Mo(CO)_6$ have been used as precursors to obtain grafted (η^6-arene) $M(CO)_3$ species inside the CPO-27-Ni material. The presence of open Ni(II) sites in the MOF scaffold promotes distinctive reactivities with respect to that observed previously on other MOFs (MOF-5 and UiO-66). The formation of two organometallic $M(CO)_3$(η^6-arene) conformers (staggered and eclipsed) has been considered, also taking into account data obtained by a recent theoretical work. IR spectroscopy shows how open metal sites in a MOF structure can destabilize metal carbonyl molecules, favoring CO elimination and acting as CO scavenger, which fastens the decomposition and frustrate the reverse reaction. The work can open new studies on precursors of catalytic species stabilized inside MOFs cages.

1. Introduction

Metal hexacarbonyls have been used extensively in the past as precursors to functionalize high surface area materials such as zeolites and oxides [1]. On account of their low sublimation temperature, metal carbonyls can be in fact dosed on different materials from the gas phase, and successively heated in controlled atmosphere with consequent surface functionalization. Examples are given in literature in respect to MgO, alumina, silica, H-ZSM-5, NaY, NaX and others [2], [3], [4], [5], [6], [7] and [8], where the adsorbed surface adducts showed a different stability as a function of the combination metal hexacarbonyls-support. In some cases, the formation of subcarbonyl species was also reported. More recently, metal hexacarbonyls have been successfully used to functionalize metal–organic framework (MOFs) and meso or microporous materials having a hybrid organic–inorganic nature. In both classes of materials, the presence of arene rings as constituents of the microporous network, combined with the stability of the (η^6-arene)$M(CO)_3$ unities opens the possibility to use $M(CO)_6$ as precursors for post-synthetic modification in view of specific applications. As an examples $Cr(CO)_6$ has been used to functionalize a silica-bonded polyphenylsiloxane resulting in a stereoselective catalyst for hydrogenation of sorbate and soybean methyl esters [9], and to functionalize an inorganic–organic hybrid mesoporous silica through grafting of the $Cr(CO)_3$ moieties on the phenylene units [10]. Very recently, Kaye and Long [11] and Chavan et al. [12]applied a similar strategy to functionalize the arene ring of the organic linker in MOF-5 and UiO-66 materials. In all cases the functionalization proceeded through a controlled thermal decomposition of $Cr(CO)_6$ precursor, according to Eq. (1), and involved porous structures that did not show other grafting centers but only the benzene rings of the linker.

Herein, we report the post synthetic functionalization, through $M(CO)_3$ moieties, of a metal–organic framework (CPO-27-Ni). The novelty of the work is due to the fact that the MOF used to graft $M(CO)_3$ moieties, is characterized by the presence of metal centers with available coordination vacancies. This is the first time that a post synthetic functionalization is performed on a MOF that can influence the chemistry of the $M(CO)_6$organometallic precursor. CPO-27-Ni (example of the class of CPO-27-M materials, [13]also termed as M_2-(DOBDC) [14] or MOF-74 [15]) is a three dimensional framework resulting from hexagonal packing of helical O_5Ni chains connected by 2,5-dihydroxyterephthalate linkers. The resulting structure shows a one-dimensional arrangement of parallel hexagonal channels, 11 Å in diameter, having the Ni^{2+} ions at the vertices of the hexagons formed by the organic linkers. All of the oxygen atoms present in the carboxylate and hydroxylate groups of the ligand coordinates the metal cation. Such geometry yields five oxygen atoms in the coordination sphere of each M^{2+} cation, which has a sixth coordination position occupied by a water molecule. The coordinated water molecule can be removed upon thermal treatment at 393 K in vacuum, leaving the metal cation with an open (accessible) coordination site that can be occupied by an adsorbed guest molecule [16]. The detailed spectroscopic characterization of solvent desorption (or dehydration) to generate coordinatively unsaturated Ni^{2+} sites and their reactivity toward various probe molecules were described elsewhere [17], [18], [19], [20] and [21]. Of particular relevance for this study is the adsorption of CO on CPO-27-Ni reported by Chavan et al. [21]. These results have shown that CO interacts strongly with Ni^{2+} and forms monocarbonylic adducts characterized by an IR absorption at 2178 cm^{-1} (blue shifted with respect to the pure physisorbed phase observed at 2138 cm^{-1}). In the present paper, the role of the coordinatively unsaturated Ni^{2+} sites in determining the adsorption and reactivity of $M(CO)_6$ (M = Cr, Mo) inside CPO-27-Ni is investigated by means of FTIR spectroscopy, which was already demonstrated to be a sensitive techniques to reveal the occurrence of $M(CO)_3$ grafting [12]. Experimental results are discussed in comparison with data obtained from molecular modeling [22]. Different reactivity and

stability inside CPO-27-Ni is observed for both precursors $M(CO)_6$ (M = Cr, Mo) and products $M(CO)_3$, as will be discussed here below.

2. Experimental

2.1. Materials

$Cr(CO)_6$, $Mo(CO)_6$ and $(C_6H_6)Cr(CO)_3$ were obtained from Aldrich and used without any further treatment.
The CPO-27-Ni material $Ni_2(dhtp)(H_2O)_2 \cdot 8H_2O$ was synthesized at 383 K from a stoichiometric solution of nickel(II) acetate and 2,5-dihydroxyterephthalic acid in a THF–water mixture, following a recipe reported in literature [13]. Powder X-ray diffraction data confirm the structure of the compound. When dehydrated at 393 K, the sample presents a BET surface area of 981 $m^2\ g^{-1}$ (Langmuir surface area of 1083 $m^2\ g^{-1}$) and pore diameter of 11–12 Å [13].

2.2. Methods

2.2.1. In situ grafting of $M(CO)_3$ moieties

Prior to dosage of metal hexacarbonyls, CPO-27-Ni was activated in vacuum at 393 K to remove all the physisorbed and coordinated water molecules. $M(CO)_6$ (M = Cr or Mo) was then dosed from the gas phase upon vacuum sublimation of the solid at room temperature. The CPO-27-Ni loaded with $M(CO)_6$ was further treated at 393 K in order to react $M(CO)_6$ with the support. The reaction temperature was chosen on account of the limited thermal stability of the matrix.

2.2.2. FTIR spectroscopy

FT-IR spectra were collected in transmission mode at 2 cm^{-1} resolution on a Bruker IFS66 spectrophotometer equipped with a DTGS (deuterated triglycine sulfate) detector. FT-IR measurements were performed on a thin layer of sample deposited on silicon disk, in order to obtain in scale FT-IR spectra also at low frequency value, where strong IR absorption bands due to framework vibrational modes appear. The sample was placed inside a homemade IR cell that allowed us to perform in situ sample activation in high vacuum (10^{-4} mbar) or in controlled atmosphere, the dosage of probe molecules through gas or vapor phase and simultaneous spectra collection. For comparison, the IR spectra of $Cr(CO)_6$ and $(\eta^6\text{–}C_6H_6)Cr(CO)_3$ in THF solution were recorded in a cell for liquid.

2.2.3. Theoretical calculations

The calculations were performed with the *Gaussian 03* software package [23] at the B3LYP level of calculation [24] and [25]. The CPO-27-Ni framework was modeled by means of *p*-$C_6H_4(COONa)_2$. For the hydrogen atoms, the standard Pople basis set supplemented by diffuse and polarizability functions 6-311++G(2d,2p) has been adopted[26] and [27]. Sodium has been modeled by means of the fully optimized triple-ζ valence basis sets proposed by Ahlrichs et al. [28] supplemented by polarization (TZVp). For all the other elements, the TZV basis set has been augmented by two sets of polarization functions derived from the original ones following an even-tempered recipe, that is by substituting the polarization orbital in the basis set with two orbitals, having respectively the coefficient doubled and halved with respect to the parent orbital. The so obtained basis sets will be indicated as TZV2p. Geometry optimization has been carried out by means of the Berny optimization algorithm with analytical gradient. No geometrical constraints have been imposed. Harmonic frequencies have been obtained by analytically determining the second derivatives of the energy with respect to the Cartesian nuclear coordinates and then transforming to mass-weighted coordinates. No scaling factor has been adopted. For further details on the calculations please refer to Ref. [22].

3. Results and discussion

3.1. FT-IR spectra of CPO-27-Ni and $M(CO)_6$

In our previous work related to the functionalization of UiO-66 with $Cr(CO)_6$, we demonstrated that FT-IR spectroscopy coupled with theoretical calculations is a very sensitive technique to prove the occurrence of arene functionalization by a metal tricarbonyl [12]. A multi technique approach based on UV–visible and XAS results complemented the FT-IR data thus confirming the traced conclusions. Because of the relative simplicity of the experimental set up necessary for FT-IR measurements, herein we explored the functionalization of CPO-27-Ni by FT-IR spectroscopy only. Before addressing the core of the experiment, the FT-IR spectra of both CPO-27-Ni matrix and $M(CO)_6$ reagent will be briefly discussed. The FT-IR spectrum of the activated CPO-27-Ni is reported in figure S1 (Supporting Information). The spectrum shows several intense absorption bands below 1650 cm^{-1}, mainly due to the vibrational modes of the carboxylate, oxo (symmetric and asymmetric C–O stretching) and the phenyl functionality of organic linkers. In the lowest frequency region (600–400 cm^{-1}) IR absorption bands assigned to vibrations of metal-oxo species are also well defined; whereas in the frequency region above 1600 cm^{-1} many combination and overtone bands appear, along with IR bands due to C–H fundamental vibrations. An extended description of the vibrational features of CPO-27-Ni is reported elsewhere [17] and [19]. For the scope of the work, it is sufficient to remember that in the 2000–1900 cm^{-1}frequency region, where the main vibrations due to $M(CO)_6$ and (η^6-arene)$M(CO)_3$appear [29], no absorption bands due CPO-27-Ni are observed.

As reported previously [29], the IR spectrum of $M(CO)_6$ (M = Cr, Mo) in the gas phase is characterized by four IR absorption bands, centered around 2000, 670, 440, and 100 cm^{-1}, which are assigned respectively to the four IR-active vibrational modes (T_{1u}symmetry): CO stretching, ν(CO); metal–carbon–oxygen bending, δ(M–C–O); metal–carbon stretching, ν(M–C) and carbon–metal–carbon deformation, def(C–M–C), respectively. Because of instrumental limitations, only the ν(CO) and δ(Cr–C–O) regions were accessible and therefore only these two IR absorption bands will be discussed hereafter. The decreased symmetry of $M(CO)_6$ species [30] in solution and in solid state results into a small shift to lower frequency of the IR absorption bands and into the appearance in the IR spectrum of some Raman-active vibrational modes(ν(CO): 2112 and 2018 cm^{-1}; δ(Cr–C–O): 436 cm^{-1}; ν(MC): 381 and 394 cm^{-1}). As an example, in the IR spectrum of $Cr(CO)_6$ dissolved in THF (Fig. 1a, gray curve) the main IR absorption bands are shifted to lower frequency with respect to the gas phase values (ν(CO) at 1979 cm^{-1} and δ(Cr–C–O) at 665 cm^{-1} vs. 2000 and 668 cm^{-1}). The Raman-active ν(CO) vibration is also visible (E_g symmetry, weak band at 2020 cm^{-1}).

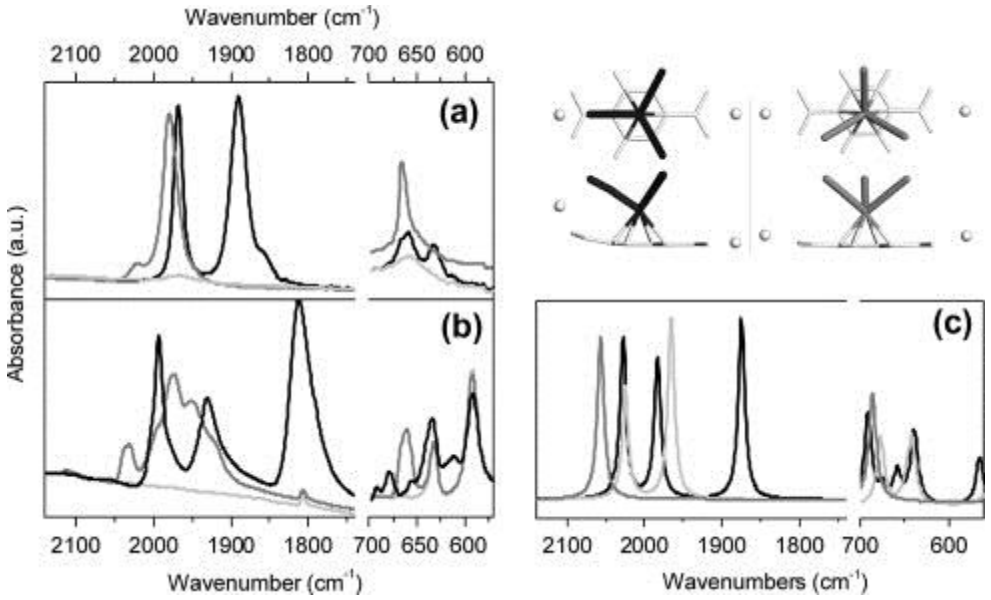

Fig. 1.

Experimental IR spectra of $Cr(CO)_6$ (gray), $(\eta^6\text{-}C_6H_6)Cr(CO)_3$ (black) in THF (part a) and in CPO-27-Ni (part b). (Part c) Computed unscaled IR spectra for the $Cr(CO)_6$ (gray), $[\eta^6\text{-}C_6H_4(COONa)_2]Cr(CO)_3$ staggered (light gray) and eclipsed (black) conformers.

Similar spectral changes are observed for $M(CO)_6$ adsorbed on a solid support, [1], [2],[4], [6], [7], [31] and [32] for which the number of IR absorption bands and the magnitude of shift for ν(CO) in comparison to $M(CO)_6$ in gas phase depend on the type of interaction between $M(CO)_6$ and the support surface. Generally speaking, metal carbonyls can interact with a surface following two different routes depending on the chemical and physical properties of the surface: *Ligand centered interaction*, where metal carbonyls are bound to the surface through the O atoms by donor–acceptor interaction with Lewis sites, hydrogen bonding with hydroxylated surface or weak physisorption on covalent surface or *Metal centered interaction* (inner sphere reactions), which mainly involve attack at the metal center and can be facilitated by primary O-bonding to the support, since this alters the electron density distribution of the metal carbonyl.

3.2. Adsorption and reactivity of $Cr(CO)_6$ onto CPO-27-Ni

The FT-IR spectrum of $Cr(CO)_6$ adsorbed on CPO-27-Ni at room temperature (gray spectrum in Fig. 1b and S2) is more complex than that of $Cr(CO)_6$ in THF solution: in fact, in addition to the main IR absorption bands at 1994, 1974 and 1951 cm^{-1} due to the IR-active CO stretching vibrations of T_{1u} symmetry, a weak IR absorption band at 2110 $cm^{-1}$and a doublet at 2040–2030 cm^{-1} were observed. These bands are assigned to the Raman active CO stretching vibrations of A_{1g} and E_g (non-degenerate) symmetry, respectively. In the low frequency region a vibration associated to δ(Cr–C–O) is observed around 662 cm^{-1} (~6 cm^{-1} red shifted from the gas value, 668 cm^{-1}). Both the splitting of the ν(CO) band in several components and the presence of intense bands due to Raman active modes, provide evidence that adsorption induced a distortion of $Cr(CO)_6$ from the perfect octahedral symmetry. Although evident also for $Cr(CO)_6$ in MOF-5 [11] and UiO-66 [12] the distortion is greater in the present case and is induced by the presence of open nickel sites. The strong binding of $Cr(CO)_6$ to CPO-27-Ni is also supported by: (i) the almost complete irreversibility upon outgassing at room temperature; (ii) the observation that CO (which is a strong probe for Ni^{2+} sites in CPO-27-Ni) is not able to displace $Cr(CO)_6$ (see Figure S3 for details and the corresponding discussion). The ordered distribution of Ni^{2+} open sites implies an ionic character of the microporous framework that acts as host for the $M(CO)_6$ units. Similar results were previously observed for $M(CO)_6$ adsorption on solid supports having unsaturated surface metal sites [2], [4], [5] and [7] and were rationalized through the interaction between the solids' Lewis sites and adsorbed $M(CO)_6$. Therefore, in analogy with these precedents, the strong interaction observed between $Cr(CO)_6$ and the CPO-27-Ni can be explained by considering the polarizing nature of the surface. Conversely, reactions with PS, UiO-66 and MOF-5 (materials with no unsaturated surface metal sites) required higher temperatures, could not be speed up by performing the thermal, and in general displayed reversible $Cr(CO)_6$ adsorption, in stark contrast with our result with CPO-27-Ni. The formation of $(\eta^6\text{-arene})Cr(CO)_3$ complexes inside CPO-27-Ni was achieved by thermal decomposition of the $Cr(CO)_6$ precursor at 393 K; the reaction conditions were milder: shorter reaction time (1 h) and lower temperature (393 K) with respect to those reported for PS, UiO-66 (423 K for 12 h), [12] and MOF-5. [11]. Moreover, since the formation of $(\eta^6\text{-arene})M(CO)_3$ complex from the precursor $M(CO)_6$ is in equilibrium with the reverse reaction of $M(CO)_6$ reformation, as shown in Eq. (1), the yield of $(\eta^6\text{-arene})M(CO)_3$complex was maximized by removing the CO released during the reaction (i.e. performing the thermal decomposition in dynamic vacuum).

equation(1)

$$Arene+M(CO)_6 \leftrightharpoons (\eta^6\text{-}Arene)M(CO)_3+3CO$$

The successful functionalization of CPO-27-Ni with $Cr(CO)_3$ is demonstrated by the disappearance in the IR spectrum, of the IR absorption bands due to adsorbed $Cr(CO)_6$and by the concomitant growth of new bands in the ν(CO) region, as shown in Fig. 1b (black curve). Three IR absorption bands are present in the ν(CO) region: a sharp and intense band at 1993 cm^{-1} showing a low frequency shoulder at 1979 cm^{-1}, a quite broad band at 1930 cm^{-1} and an intense and broader band at 1812 cm^{-1}. The IR spectrum of the highly symmetric $(\eta^6\text{-}C_6H_6)Cr(CO)_3$ (Fig. 1a, black curve) shows two IR absorption bands in the ν(CO) region, at 1968 and 1890 cm^{-1}, which are assigned to the non-degenerate total symmetric stretching $\nu(CO_{totsym})$ and to the doubly degenerate total asymmetric stretching $\nu(CO_{asym})$ respectively [22] and [33]. The presence of three IR absorption bands in the ν(CO) region for $Cr(CO)_3$ grafted on CPO-27-Ni suggests the rupture of the quasi-degeneracy of the asymmetric stretching modes, due to the interaction of the CO molecules with the exposed Ni^{2+} ions.
These results are supported by the previous calculations on $[\eta^6C_6H_4(COONa)_2]Cr(CO)_3$[22] where the Na^+ cations were chosen to simulate the effect of open metal sites nearby the $Cr(CO)_3$ tripod. Among the two possible conformers (staggered and eclipsed, see inset in Fig. 1c) for $[\eta^6\text{-}C_6H_4(COONa)_2]Cr(CO)_3$ the minimum conformation was found to be the eclipsed one, opposite to what found for the parent complexes $(\eta^6\text{-}C_6H_6)Cr(CO)_3$ and $[\eta^6\text{-}C_6H_4(COOH)_2]Cr(CO)_3$[22]. The higher stability of the eclipsed conformer would result from the mobility of the Na^+ cation that, after the formation of $Cr(CO)_3$ complex with arene ring of the linker, moves from its original position in order to interact with the negatively charged O atoms of the $Cr(CO)_3$ unit. The computed IR spectra of the $[\eta^6\text{-}C_6H_4(COONa)_2]Cr(CO)_3$ model in the staggered (light gray) and eclipsed (black) conformations are compared in Fig. 1c. The computed spectrum for the staggered conformer shows only two absorption bands at 2025 and 1983 cm^{-1}, whereas the IR spectrum of the eclipsed conformer shows an additional IR absorption band at 1860 cm^{-1}. The latter is due to the simultaneous interaction of one CO molecule with the Cr center (through the C atom) and the Na^+ center (through the O atom). The corresponding ν(CO) is in fair agreement with that of the most red-shifted IR absorption band in the spectrum of $(CPO\text{-}27\text{-}Ni)Cr(CO)_3$ (1812 cm^{-1}), providing evidence that this band is originated by the direct interaction of one CO of the $Cr(CO)_3$ tripod with the exposed Ni^{2+} ion through the O atom. Hence, the IR absorption band at 1993 cm^{-1} in the spectrum of $(CPO\text{-}27\text{-}Ni)Cr(CO)_3$ (Fig. 1b, black curve) is assigned to the total symmetric stretching of the three CO molecules ($\nu(CO_{totsymm})$), and the IR absorption bands centered at 1939 and 1812 cm^{-1} to the asymmetric modes of the three CO $(\nu(CO)_{asymm})$.
As a conclusion of this section, IR spectroscopy demonstrated that, despite the milder conditions, a faster reactivity is observed for $Cr(CO)_6$ in CPO-27-Ni compared to $Cr(CO)_6$in PS, UiO-66 [12] and MOF-5 [11]. The higher reactivity can be attributed to the presence of open Ni(II) sites, which play three important roles. First of all, the presence of Ni(II) sites determines a strong binding of $Cr(CO)_6$ which is not removed by outgassing, neither displaced by incoming CO. Secondly, Ni(II) sites destabilize metal carbonyl molecules (as discussed above), favoring CO elimination. Destabilization of $Cr(CO)_6$ is proved by the corresponding IR spectrum, showing several IR absorption bands in the ν(CO) region, which provide evidence that adsorption induces distorption of $Cr(CO)_6$. Finally, the open Ni(II) sites act as CO scavenger which fasten the decomposition and frustrate the reverse reaction. This latter role (CO scavenger) is further demonstrated by the appearance in the IR spectrum of CPO-27-Ni heated in presence of $Cr(CO)_6$ (in closed cell) of an IR absorption band at 2178 cm^{-1}, which is associated to CO adsorbed on Ni(II) sites (figure S2) [21].

3.3. Adsorption and reactivity of $Mo(CO)_6$ onto CPO-27-Ni

A parallel study was performed using $Mo(CO)_6$ as functionalizing molecule. The FT-IR spectrum of $Mo(CO)_6$ adsorbed on CPO-27-Ni activated at 393 K is shown in Fig. 2 (gray curve). the molybdenum(0) hexacarbonyl $Mo(CO)_6$ is likewise almost irreversibly adsorbed at room temperature on CPO-27-Ni. Similarly to $Cr(CO)_6$, the IR spectrum of adsorbed $Mo(CO)_6$ shows characteristic IR absorption bands that provide evidence of molecule distortion. In particular, the decreased symmetry is evidenced by the presence of additional IR absorption bands besides those

due to ν(CO), whose intensity is above saturation: a band at 2115 cm^{-1} and a doublet at 2043 and 2028 cm^{-1} assigned to the Raman active A_{1g} and E_g vibrational modes, respectively.

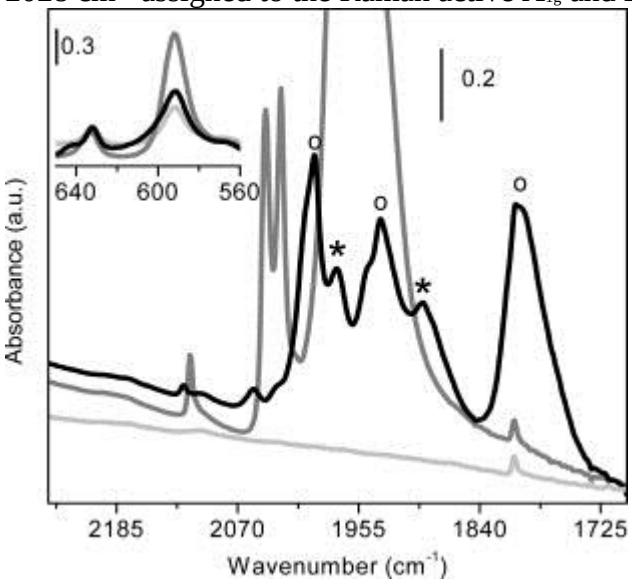

Fig. 2.
FTIR spectra of CPO-27-Ni activated (light gray curve), $Mo(CO)_6$ (gray curve) and (η^6-arene)$Mo(CO)_3$(black curve). The inset reports the bending region of carbonyl complexes. Circles and asterisks mark the peaks corresponding to the eclipsed and staggered conformers, respectively.

The thermal decomposition of $Mo(CO)_6$ in CPO-27-Ni has been performed following the same procedure discussed for $Cr(CO)_6$, and the resulting FT-IR spectrum is shown inFig. 2 (black curve). The IR absorption band characteristic of adsorbed $Mo(CO)_6$disappears with the concomitant formation of a complex IR spectrum, where five main components can be distinguished. In particular, new IR absorption band at 1997 cm^{-1}, a minor band at 1976 cm^{-1}, a broad and complex absorption at 1934 cm^{-1} accompanied by a minor band at 1895 cm^{-1} and an intense IR absorption band at 1804 cm^{-1} are observed. In analogy to the chromium system discussed above, the main bands at 1997, 1934 and 1804 cm^{-1} (peaks marked with a circle in Fig. 2) can be associated to the eclipsed form of the tripod. In particular the IR component at 1997 cm^{-1} is ascribed to the total symmetric stretching $\nu(CO)_{totsymm}$, while the doublet at 1934 and 1804 cm^{-1} is due to the asymmetric modes of the tricarbonyl $\nu(CO)_{asymm}$. The presence of the two additional bands at 1976 cm^{-1}, and at 1895 cm^{-1} (peaks marked with an asterisks in Fig. 2) can be justified by considering the formation of the staggered conformer, for which a doublet is expected (see part c of Fig. 1 and the description of the computational part). This assignment implies that in case of the (η^6-arene)$Mo(CO)_3$ complex, although the eclipsed conformer remains the most abundant, the staggered one is present, indicating that the relative stability of the two conformers is different for molybdenum vs. chromium complexes.

3.4. Reversibility of the (η^6-arene)$M(CO)_3$ complex

The stability of the formed (η^6-arene)$M(CO)_3$ complexes inside CPO-27-Ni was checked with respect to CO at room temperature. Fig. 3 shows the FT-IR spectra obtained for successive CO dosages on CPO-27-Ni functionalized with $Cr(CO)_3$ (part a) and $Mo(CO)_3$ (part b) species. The (η^6-arene)$Cr(CO)_3$ moieties are found to be pretty stable and no changes in the FT-IR spectrum of (η^6-arene)$Cr(CO)_3$ is observed after the addition of CO (bold gray curve, 16 mbar). On the contrary, the IR spectrum of (η^6-arene)$Mo(CO)_3$ complex significantly changes, even for a small addition of CO (gray curve 10 mbar). In particular the IR absorption band at 1804 cm^{-1} decreases in intensity, indicating that CO molecules partially displaces the formed complexes from the accessible Ni^{2+} sites. In parallel, the spectra show even more complex shape due to the growth of IR absorption bands at 2032 cm^{-1}, 1968 cm^{-1}, 1935 and 1899 cm^{-1}. All these features suggest a partial restoration of the original $Mo(CO)_6$ complex.

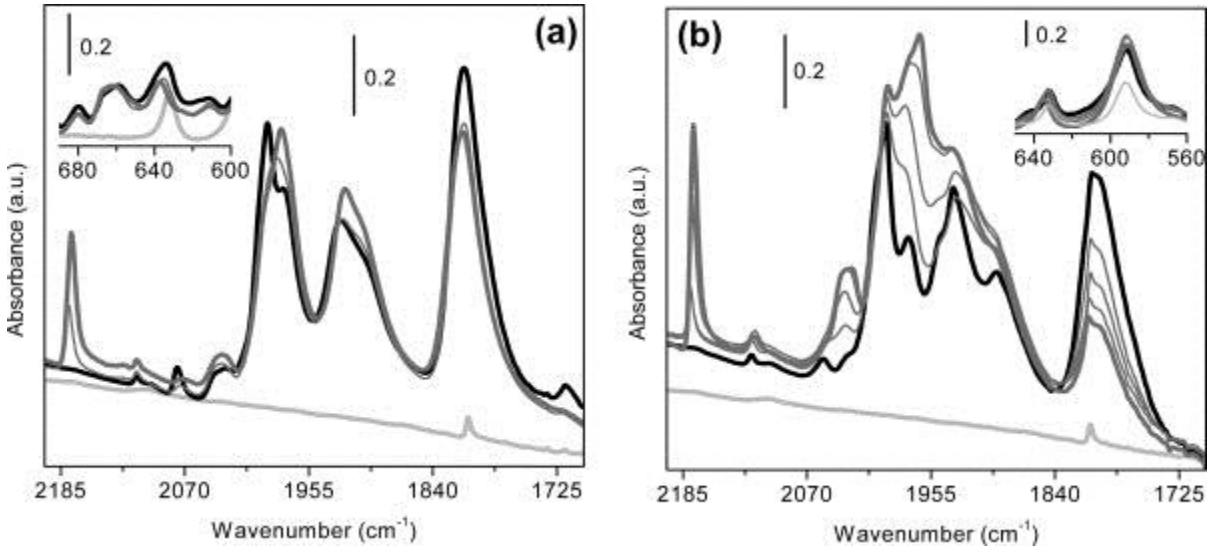

Fig. 3.
Reversibility in the presence of CO of the reaction reported in Eq. (1) for $Cr(CO)_6$ (a) and $Mo(CO)_6$ (b). Light gray curve: spectrum of matrix before dosage of $M(CO)_6$; black curve: anchored (η^6-arene)$M(CO)_3$; gray curve: evolution upon CO dosage. Inset is showing the bending region of the carbonyl complexes.

4. Conclusions

$M(CO)_6$ adsorption inside CPO-27-Ni, and its successive thermal decomposition leading to grafted $M(CO)_3$ species have been investigated by in situ IR spectroscopy revealing a distinctive reactivity with respect to the predecessor MOF-5 and UiO-66. Spectroscopically it has been shown how the open site in a MOF can induce a very peculiar spatial organization of the grafted moiety. The faster and stronger reactivity observed for $M(CO)_6$ in CPO-27-Ni compared to that found in PS, UiO-66 and MOF-5[11] and [12], can be attributed to the presence of open Ni(II) sites, that play an important dual role. First of all, Ni(II) sites destabilize metal carbonyl molecules favoring CO elimination and subsequent formation of surface-bonded subcarbonyl adducts and secondly they act as CO scavenger, which fastens the decomposition and frustrates the reverse reaction.
In agreement with theoretical work recently published, the concomitant presence of two conformers for the grafted organometallic moiety (η^6-arene)$M(CO)_3$, corresponding to the staggered and eclipsed conformers has been evidenced. The presence of a strong interaction between one carbonyl ligand and the acid site (the open Ni(II) site in the MOF scaffold) favors the formation of the eclipsed form. The eclipsed conformer is the only species evidenced in case of (η^6-arene)$Cr(CO)_3$ complex, while for (η^6-arene)$Mo(CO)_3$species, the staggered form was also observed.

Acknowledgments

Financial support by European VI framework through STREP project MOFCAT Contract number: NMP4-CT-2006-033335 is gratefully acknowledged. Elena Groppo and Carlo Lamberti are acknowledged for fruitful discussions.

References

[1] E. Guglielminotti, J. Mol. Catal. 13 (1981) 207.

[2] E. Guglielminotti, A. Zecchina, Journal de chimie physique 78 (1981) 11.

[3] Y. You-Sing, R.F. Howe, J. Chem. Soc. Faraday Trans. I 82 (1986) 2887.

[4] A. Zecchina, E.E. Platero, C.O. Arean, Inorg. Chem. 27 (1988) 102.

[5] Y. Okamato, A. Maezawa, H. Kane, I. Mitsushima, T. Imanaka, J. Chem. Soc. Faraday Trans. 1 (84) (1988) 851.

[6] A. Zecchina, M.K. Rao, S. Coluccia, E.E. Platero, C.O. Arean, J. Mol. Catal. 53 (1989) 397.

[7] A. Zecchina, C.O. Arean, Catal. Rev.-Sci. Eng. 35 (1993) 261.

[8] G. Hunter, C.H. Rochester, A.G. Wilkinson, J. Paton, J. Chem. Soc. Faraday Trans. 92 (1996) 5093.

[9] R.A. Awl, E.N. Frankel, JAOCS (1981) 557.

[10] T. Kamegawa, T. Sakai, M. Matsuoka, M. Anpo, J. Am. Chem. Soc. 127 (2005) 16784.

[11] S.S. Kaye, J.R. Long, J. Am. Chem. Soc. 130 (2008) 806.

[12] S. Chavan, J.G. Vitillo, M.J. Uddin, F. Bonino, C. Lamberti, E. Groppo, K.-P. Lillerud, S. Bordiga, Chem. Mater. 22 (2010) 4602.

[13] P.D.C. Dietzel, B. Panella, M. Hirscher, R. Blom, H. Fjellvag, Chem. Commun. (2006) 959.

[14] S.R. Caskey, A.G. Wong-Foy, R.A.J. Matzger, J. Am. Chem. Soc. (2008) 10870.

[15] N.L. Rosi, J. Kim, M. Eddaoudi, B. Chen, M. O'Keeffe, O.M. Yaghi, J. Am. Chem. Soc. 127 (2005) 1504.

[16] P.D.C. Dietzel, R.E. Johnsen, R. Blom, H. Fjellvag, Chem. Eur. J. 14 (2008) 2389.

[17] F. Bonino, S. Chavan, J.G. Vitillo, E. Groppo, G. Agostini, C. Lamberti, P.D.C. Dietzel, C. Prestipino, S. Bordiga, Chem. Mater. 20 (2008) 4957.

[18] J.G. Vitillo, L. Regli, S. Chavan, G. Ricchiardi, G. Spoto, P.D.C. Dietzel, S. Bordiga, A. Zecchina, J. Am. Chem. Soc. 130 (2008) 8386.

[19] S. Chavan, F. Bonino, J.G. Vitillo, E. Groppo, C. Lamberti, P.D.C. Dietzel, A. Zecchina, S. Bordiga, Phys. Chem. Chem. Phys. 11 (2009) 9811.

[20] P.D.C. Dietzel, R.E. Johnsen, H. Fjellvag, S. Bordiga, E. Groppo, S. Chavan, R. Blom, Chem. Commun. (2008) 5125.

[21] S. Chavan, J.G. Vitillo, E. Groppo, F. Bonino, C. Lamberti, P.D.C. Dietzel, S. Bordiga, J. Phys. Chem. C (2009) 3292.

[22] J.G. Vitillo, E. Groppo, S. Bordiga, S. Chavan, G. Ricchiardi, A. Zecchina, Inorg. Chem. 48 (2009) 5439.

[23] M.J. Frisch, G.W. Trucks, H.B. Schlegel, G.E. Scuseria, M.A. Robb, J.R. Cheeseman, J. Montgomery, J. A., T. Vreven, K.N. Kudin, J.C. Burant, J.M. Millam, S.S. Iyengar, J. Tomasi, V. Barone, B. Mennucci, M. Cossi, G. Scalmani, N. Rega, G.A. Petersson, H. Nakatsuji, M. Hada, M. Ehara, K. Toyota, R. Fukuda, J. Hasegawa, M. Ishida, T. Nakajima, Y. Honda, O. Kitao, H. Nakai, M. Klene, X. Li, J.E. Knox, H.P. Hratchian, J.B. Cross, V. Bakken, C. Adamo, J. Jaramillo, R. Gomperts, R.E. Stratmann, O. Yazyev, A.J. Austin, R. Cammi, C. Pomelli, J.W. Ochterski, P.Y. Ayala, K. Morokuma, G.A. Voth, P. Salvador, J.J. Dannenberg, V.G. Zakrzewski, S. Dapprich, A.D. Daniels, M.C. Strain, O. Farkas, D.K. Malick, A.D. Rabuck, K. Raghavachari, J.B. Foresman, J.V. Ortiz, Q. Cui, A.G. Baboul, S. Clifford, J. Cioslowski, B.B. Stefanov, G. Liu, A. Liashenko, P. Piskorz, I. Komaromi, R.L. Martin, D.J. Fox, T. Keith, M.A. Al-Laham, C.Y. Peng, A. Nanayakkara, M. Challacombe, P.M.W. Gill, B. Johnson, W. Chen, M.W.Wong, C. Gonzalez and J.A. Pople, Gaussian 03, Revision B. fifth ed.Gaussian, Inc., Wallingford CT, 2004. [24] C. Lee, W. Yang, R.G. Parr, Phys. Rev. B 37 (1988) 785.

[25] A.D. Becke, J. Chem. Phys. 98 (1993) 5648.

[26] T. Clark, J. Chandrasekhar, G.W. Spitznagel, P.v.R. Schleyer, J. Comput. chem. 4 (1983) 294.

[27] M.J. Frisch, J.A. Pople, J.S. Binkley, J. Chem. Phys. 80 (1984) 3265.

[28] A. Schäfer, C. Huber, R. Ahlrichs, J. Chem. Phys. 100 (1994) 5829.

[29] D.M. Adams, Metal-Ligand and Related Vibrations, Edward Arnold Ltd, London, 1967.

[30] D.A. Kariuki, S.F.A. Kettle, Inorg. Chem. 17 (1978) 141.

[31] B. Fubini, E. Giamello, E. Guglielminotti, A. Zecchina, J. Mol. Catal. 32 (1985) 219.

[32] E.E. Platero, C.O. Arean, D. Scarano, G. Spoto, A. Zecchina, Mater. Chem. Phys. 29 (1991) 347.

[33] A. Berces, T. Ziegler, J. Phys. Chem. 98 (1994) 13233.